Cluster percolation in $O(n)$ spin models

2000 J. Phys. A: Math. Gen. 33 8603

(http://iopscience.iop.org/0305-4470/33/48/301)

J. Phys. A: Math. Gen. **33** (2000) 8603–8613. Printed in the UK PII: S0305-4470(00)15935-9

Cluster percolation in $O(n)$ spin models

Ph Blanchard†, S Digal†, S Fortunato†, D Gandolfo‡, T Mendes† and H Satz†

† Fakultät für Physik, Universität Bielefeld, D-33615, Bielefeld, Germany
‡ Dépt de Math., Université de Toulon et du Var, F-3957 La Garde Cedex, France
and
CPT, CNRS, Luminy, case 907, 13288 Marseille Cedex 09, France

Received 28 July 2000, in final form 17 October 2000

Abstract. The spontaneous symmetry breaking in the Ising model can be equivalently described in terms of percolation of Wolff clusters. In $O(n)$ spin models similar clusters can be built in a general way, and they are currently used to update these systems in Monte Carlo simulations. We show that for three-dimensional $O(2)$, $O(3)$ and $O(4)$ such clusters are indeed the physical 'islands' of the systems, i.e. they percolate at the physical threshold and the percolation exponents are in the universality class of the corresponding model. For $O(2)$ and $O(3)$ the result is proven analytically, for $O(4)$ we derived it by numerical simulations.

1. Introduction

The possibility to interpret the critical behaviour of dynamical systems in terms of percolation of geometrical structures of the system has always had a great appeal in the study of critical phenomena [1, 2]. Attempts in this direction had already begun by the 1970s, when the behaviour of clusters of nearest-neighbour like-signed spins started to be studied using the Ising model. It turned out that in two dimensions these elementary site percolation clusters do indeed undergo a geometrical transition exactly at the critical threshold of the Ising model [3]. This result, which is not valid in three dimensions [4], is not so appealing because the critical exponents derived by the percolation variables do not coincide with the Ising ones [5]. The correspondence between the geometrical and the thermal phenomenon is therefore only partial.

The problem was solved by Coniglio and Klein [2], making use of a different definition for the clusters. Such a definition had already been used by Fortuin and Kasteleyn to show that the partition function of the Ising model can be rewritten in purely geometrical terms as a sum over cluster configurations [6]. According to the Fortuin–Kasteleyn prescription, two nearest-neighbour spins of the same sign belong to the same cluster with probability $p = 1 - \exp(-2\beta)$ ($\beta = J/kT$, where J is the Ising coupling). Coniglio and Klein [2] showed that the geometrical transition of these clusters leads to the required critical indices of the Ising model (threshold and exponents).

The clusters of the Monte Carlo cluster update introduced by Wolff [7] for $O(n)$ spin models coincide with the Fortuin–Kasteleyn ones when $n = 1$ (which is just the Ising model). The $O(n)$ models without an external field in three space dimensions ($n \geqslant 2$) undergo a phase transition due to the spontaneous breaking of the continuous rotational symmetry of their Hamiltonian. Such models are very interesting: some physical systems in condensed matter physics are directly associated with them. The three-dimensional $O(3)$ model is the

0305-4470/00/488603+11$30.00

low-temperature effective model for a bidimensional quantum antiferromagnet [8]. The $O(2)$ model in three dimensions is known to be in the same universality class as superfluid ^{4}He. $O(n)$ models are also very useful for studying relativistic field theories. The $O(4)$ model in three dimensions has been conjectured to be in the same universality class as the finite-temperature chiral phase transition of quantum chromodynamics with two flavours of massless quarks [9].

The general definition of Wolff clusters for $O(n)$ spin models inspired this work. Can one describe the critical behaviour of $O(n)$ without a field in three dimensions in terms of the percolation of these clusters, as in the $n = 1$ case? We will show that this is indeed true at least for $O(2)$, $O(3)$ and $O(4)$. The fact that the Wolff clusters percolate at the physical critical point was recently proven analytically for $O(2)$ and $O(3)$ [10, 11]. Although nothing concerning the exponents was mentioned, we will show that starting from some relations established in [10, 11] it is also possible to deduce the equality of the critical exponents for $O(2)$ and $O(3)$. We have also performed computer simulations on $O(2)$ and $O(4)$ in order to illustrate this result for $O(2)$, and to prove it numerically for $O(4)$.

2. $O(n)$ models and Wolff clusters

The $O(n)$ spin models with no external magnetic field have the following Hamiltonian:

$$H = -J \sum_{\langle i,j \rangle} \boldsymbol{s}_i \boldsymbol{s}_j \tag{2.1}$$

where i and j are nearest-neighbour sites on a d-dimensional hypercubic lattice, and $\boldsymbol{s}_i$ is an n-component unit vector at site i (J is the coupling). The partition function of these models at temperature T is

$$Z(T) = \int \mathcal{D}[\boldsymbol{s}] \exp\left\{ \beta \sum_{\langle i,j \rangle} \boldsymbol{s}_i \boldsymbol{s}_j \right\} \tag{2.2}$$

where $\beta = J/kT$ and the integral is extended over all spin configurations $\{\boldsymbol{s}\}$ of the system. In three dimensions the $O(n)$ models undergo a second-order phase transition. The order parameter of this transition is the normalized magnetization $M = \frac{1}{V} \sum_i \boldsymbol{s}_i$ (where V is the lattice volume).

Numerical simulations of $O(n)$ models became much quicker and more effective after Wolff [7] introduced a Monte Carlo algorithm based on simultaneous updates of large clusters of spins, generalizing the Swendsen–Wang algorithm [12] to the continuous-spin case. This algorithm has the remarkable advantage that it eliminates the problem of critical slowing down, an effect that makes simulations around criticality very lengthy with traditional local methods (Metropolis, heat bath). The Wolff algorithm can be basically divided into two phases:

1. a cluster of spins is selected;
2. the spins of this cluster are 'flipped', i.e. they are reflected with respect to some defined hyperplane.

For details of the flipping procedure see [7]. Here we are interested in the way to build up the clusters. We can split this procedure into two steps:

(a) choose a random n-component unit vector $\boldsymbol{r}$;
(b) bind together pairs of nearest-neighbour sites i, j with probability

$$p(i, j) = 1 - \exp\left\{ \min[0, -2\beta(\boldsymbol{s}_i \cdot \boldsymbol{r})(\boldsymbol{s}_j \cdot \boldsymbol{r})] \right\}. \tag{2.3}$$

From this prescription it follows that if the two spins at two nearest-neighbour sites i and j such that their projections onto the random vector $\boldsymbol{r}$ are of opposite signs, they will never belong to the same cluster ($p(i, j) = 0$). The random vector $\boldsymbol{r}$, therefore, divides the spin space into two hemispheres, separating the spins which have a positive projection onto it from those which have a negative projection. The Wolff clusters are made out of spins which all lie either in one or the other hemisphere. In this respect, we can again speak of 'up' and 'down' spins, as for the Ising model. In addition to that, the bond probability is local, since it depends explicitly on the spin vectors $\boldsymbol{s}_i$ and $\boldsymbol{s}_j$, and not only on the temperature as for the Fortuin–Kasteleyn factor.

The analogies with the Ising model are however clear, motivating the attempt to study the percolation properties of these clusters.

3. Percolation exponents for $O(2)$ and $O(3)$

In [10, 11, 13] the random-cluster representations of $O(n)$ models, $n = 2, 3$ have been derived (and exploited) through the Fortuin–Kasteleyn transformation [6] of the Hamiltonians and similar results were obtained in [14] for the continuous (or classical) spin model [15]. Wolff random cluster probability distributions [7] for these models have been studied and several monotonicity properties of these distributions (FKG properties) [16] have been established, leading to the proof of the equivalence between the onset of magnetic ordering in the $O(n)$ models ($n = 2, 3$) and percolation in the corresponding random Wolff cluster models. From the results stated above follows in a natural way the equality of the critical thermal and geometrical exponents.

In what follows we focus our attention on two variables.

- The *percolation strength* P, defined as the probability that a lattice site picked up at random belongs to the percolating cluster. P is the *order parameter* of the percolation transition.
- The *average cluster size* S, defined as

$$S = \frac{\sum_s n_s s^2}{\sum_s n_s s}.$$

  Here, n_s is the number of clusters of size s per lattice site (i.e. divided by the lattice volume) and the sums exclude the percolating cluster (see [17]).

We stress that in some cases one speaks of average cluster size referring to the average size of *all* clusters, including the percolating one. This definition makes the variable infinite above the percolation threshold. Below the threshold the two definitions obviously coincide and therefore they share the same critical exponent.

In [10, 11, 13, 14], it was proved that if $P(T)$ is the percolation strength in the random Wolff cluster representation and $m(T)$ is the magnetization in the $O(n)$ spin system, then there exists a function $c(T) \in C^\infty(\mathbb{R}^+)$ such that

$$P(T) \geqslant m(T) \geqslant c(T)\, P(T). \tag{3.1}$$

Similarly, denoting by $S(T)$ the average size of the Wolff clusters and $\chi(T)$ the (linear response) susceptibility, it was also proved that

$$S(T) \geqslant \chi(T) \geqslant c(T)^2 S(T) \tag{3.2}$$

where $c(T)$ is the same $C^\infty(\mathbb{R})$ function as in (3.1).

From scaling theory (see [18]), near criticality, the susceptibility is believed to behave according to the following law:

$$\chi(T) \underset{T\to T_c^+}{\sim} (T - T_c)^{-\gamma} \tag{3.3}$$

and the average mean cluster size of Wolff clusters should follow the law

$$S(T) \underset{T\to T_c^+}{\sim} |p(T) - p(T_c)|^{-\gamma'} \tag{3.4}$$

where $p(T)$ is the bond occupation probability in the Wolff random cluster model (i.e. the Coniglio–Klein [2] bond probability) given by $p(T) \sim 1 - \exp(-a/T)$, where a does not depend on T.

From [10, 11, 13, 14] the equality of the critical exponents γ and γ' follows readily. Indeed, because of monotonicity, taking the logarithm in (3.3) and (3.4), and using (3.2) one finds

$$-\gamma' \log|p(T) - p(T_c)| \geqslant -\gamma \log(T - T_c) \geqslant 2\log c(T) - \gamma' \log|p(T) - p(T_c)| \tag{3.5}$$

which reduces to

$$\gamma' \geqslant \gamma \frac{\log(T - T_c)}{\log|p(T) - p(T_c)|} \geqslant \gamma' - \frac{2\log c(T)}{\log|p(T) - p(T_c)|}. \tag{3.6}$$

Now when $T \to T_c^+$ and since $c(T) \in C^\infty(\mathbb{R})$, the last term vanishes and it is easy to see that $\log(T - T_c)/\log|p(T) - p(T_c)| \to_{T\to T_c^+} 1$. When $T \to T_c^+$ we get the result $\gamma = \gamma'$.

Using (3.1) and the scaling behaviours of the magnetization and the percolation strength in terms of their critical exponents β and β', respectively, one can show (following the same lines as before) that $\beta = \beta'$ when $T \to T_c^+ \equiv p(T) \to p(T_c)^+$, where $p(T)$ is again the Coniglio–Klein bond probability already defined above.

Namely, the percolation strength is believed to behave [18] as a function of the elementary bond occupation probability p according to the following law:

$$P(p) \underset{p\to p_c^+}{\sim} (p - p_c)^{\beta'} \qquad p \equiv p(T) \tag{3.7}$$

whereas, the magnetization should behave as

$$m(T) \underset{T\to T_c^-}{\sim} (T_c - T)^{\beta} \tag{3.8}$$

then using the same procedure as below, we are led to the following expression:

$$\beta' \leqslant \beta \frac{\log(T_c - T)}{\log(p(T) - p(T_c))} \leqslant \beta' - \frac{\log c(T)}{\log(p(T) - p(T_c))} \tag{3.9}$$

which, using

$$\log(T_c - T)/\log(p(T) - p(T_c)) \underset{T\to T_c^-}{\to} 1$$

and

$$\log c(T)/\log(p(T) - p(T_c)) \underset{T\to T_c^-}{\to} 0$$

gives

$$\beta = \beta'.$$

as claimed.

Concerning eventual extensions of analytical results to other spin models, we mention that the equivalence of the thermal and the geometrical phase transitions is true for $Z(3)$ and $Z(4)$ models as a consequence of the equivalences already established for the continuous spin Ising model and $O(2)$ [10, 14]. As for $O(n)$ models with $n > 3$, we note that the proof for $O(3)$ was derived starting from the result for $O(2)$. However, some additional conditions remain to be proved in order to be able to extend the result from $O(n-1)$ to $O(n)$ if $n > 3$.

4. Numerical results

We have investigated numerically the three-dimensional $O(2)$ and $O(4)$ models by performing computer simulations for several lattice sizes. The Monte Carlo update was performed using the Wolff algorithm, described in section 2. At the end of an iteration, the percolation strength P and the average cluster size S were measured. This has been done for each of the models using two different approaches.

The *first approach* is the traditional one, based on a complete analysis of the lattice configuration. Once we have the configuration we want to analyse, we build Wolff clusters until all spins are set into clusters. We assign to P the value zero if there is no percolating cluster, the ratio between the size of the percolating cluster and the lattice volume otherwise. We calculate S using the standard formula (3.1). The operational definition of a percolating cluster was taken as follows. We say that a cluster percolates if it spans the lattice from a face to the opposite one in each of the three directions x, y, z. We made this choice to reduce the possibility that, due to the finite size of the lattices, one could find more than a spanning cluster, making the definition of our variables ambiguous†.

In this approach we have used free boundary conditions.

The *second approach* is based on a single-cluster analysis. Basically, one studies the percolation properties of the cluster built during the update procedure. For the cluster building we have considered periodic boundary conditions. Suppose that s_c is the size of the cluster we built. If it percolates, we assign a value of one to the strength P and zero to the size S; otherwise, we write zero for P and s_c for S. These definitions of P and S look different from the standard definitions we have introduced above, but it is easy to see that they are equivalent to them.

In fact, we built the cluster starting from a lattice site taken at random. In this way, the probability that the cluster percolates (expressed by the new P) coincides with the probability that a site taken at random belongs to the percolating cluster (the standard definition of P). As far as the average cluster size is concerned, we can repeat the same reasoning: the probability that the cluster we built is a non-percolating cluster of size s_c is just the probability w_{s_c} that a randomly selected lattice site belongs to a non-percolating cluster of size s_c; w_{s_c} is given by

$$w_{s_c} = n_{s_c}\, s_c. \tag{4.1}$$

Because of that, whenever we find a non-vanishing size s_c, such a value will be weighted by the probability w_{s_c} in the final average S, which is then given by the following formula:

$$S = \sum_{s_c} w_{s_c} s_c = \sum_{s_c} n_{s_c}\, s_c^2 \tag{4.2}$$

where the sum runs over the non-percolating clusters. We note that equation (4.2) coincides with equation (3.1), apart from the denominator $\sum_s n_s\, s$, which is just the density of the sites belonging to finite clusters. Since this term does not contribute to the divergence of the average cluster size, the power-law behaviour of the two S's at criticality is identical, so that the critical exponent γ is the same in both cases.

As we have said, in the second approach we select a single cluster at a time from the whole configuration. Because of that we now have some freedom in choosing the definition of the percolating cluster, as we do not risk, like in the first approach, finding more spanning

† In three dimensions even this definition of a spanning cluster does not exclude the possibility of having more than one of such cluster for the same configuration. Nevertheless, the occurrence of such cases is so rare that we can safely ignore them.

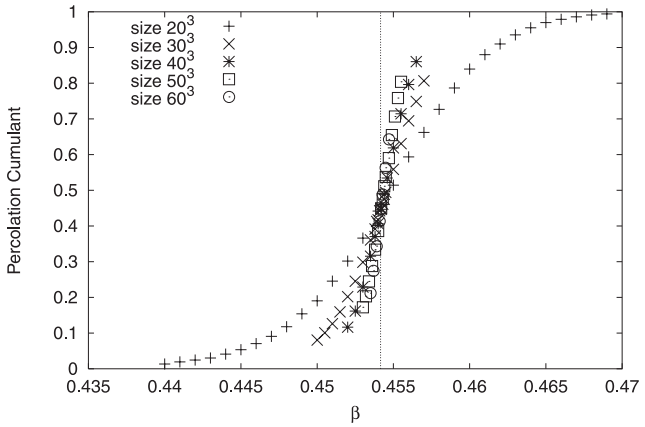

Figure 1. Percolation cumulant as a function of β for $O(2)$ and five lattice sizes. The broken line indicates the position of the thermal threshold [20].

structures. We say that the cluster percolates if it connects at least one face with the opposite one.

In this way, the definitions of percolating clusters are also different in the two approaches. This certainly influences the results on finite lattices, but has no effect on the infinite-volume properties we are interested in. In fact, it is known that one can have at most a unique spanning cluster above the critical density p_c (in our case below the critical temperature T_c). Exactly at p_c (T_c) there is a finite probability of having more than one spanning cluster [19]. So, the two different definitions of a percolating cluster we have adopted can lead to differences between the infinite-volume values *only* at the critical point p_c (T_c). However, the critical exponents are, of course, not influenced by that, as they are determined by the behaviour of the percolation variables *near* the critical point, not exactly at p_c (T_c).

The second approach has the advantage that it does not require a procedure to reduce the configuration of the system to a set of clusters; on the other hand, since it gets information from a single cluster, it requires a higher number of samples in order to measure the percolation variables with the same accuracy as the first method. Nevertheless, the iterations are faster due to the simpler measurement of observables, and are less correlated than in the first approach, since only a (random) limited region of the lattice is considered in each sample. We find that both methods are efficient, and that it is important to be able to compare results obtained in two such different ways.

For our numerical investigations we have also made use of another variable which can be extracted from the percolation strength P. On a finite lattice there is at any temperature β a well defined probability of having a spanning cluster. We call it the percolation cumulant and denote it by γ_r. When the size of the lattice goes to infinity, γ_r as a function of β approaches a step function: it is always zero below β_c and always one above it. To obtain the finite-size curves out of our measurements we must basically see how often we find a percolating cluster ($P \neq 0$) for a definite lattice size and a temperature β.

To evaluate the thresholds and the exponents we have adopted finite-size-scaling techniques. We consider the general finite-size-scaling prediction for an observable $\mathcal{O}$,

$$\mathcal{O}(t, L) = L^{\rho/\nu}\, Q_{\mathcal{O}}(L^{1/\nu} t) \tag{4.3}$$

where $t = T - T_c$, L is the linear dimension of the lattice, $Q_{\mathcal{O}}$ is a universal function and

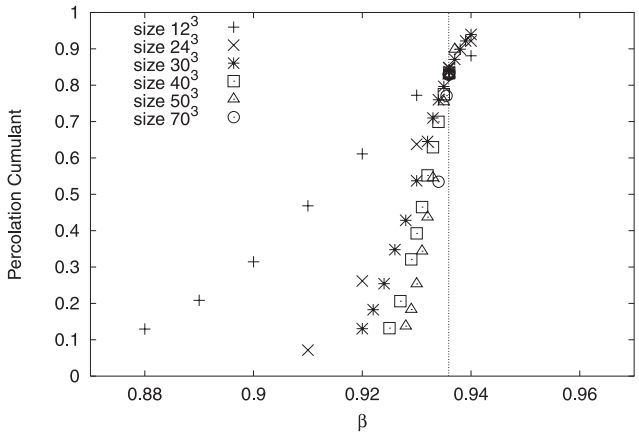

Figure 2. Percolation cumulant as a function of β for $O(4)$ and six lattice sizes. The broken line indicates the position of the thermal threshold [21].

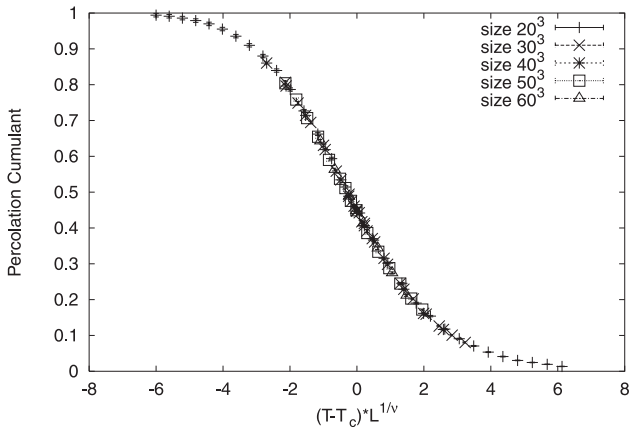

Figure 3. Rescaled percolation cumulant for $O(2)$ using $\beta_c = 0.454\,16$ and the $O(2)$ exponent $\nu = 0.672$.

the exponent ρ is related to the critical behaviour of $\mathcal{O}$ at infinite volume. Following the definitions given in section 3, we have $\rho = \gamma'$ for the observable S and $\rho = -\beta'$ for P. For the percolation cumulant γ_r we have $\rho = 0$ [18], which means that γ_r curves corresponding to different lattice sizes cross at the critical point: for $t = 0$ and $\rho = 0$, in fact, the observable of equation (4.3) is not L dependent.

Figures 1 and 2 show γ_r curves for $O(2)$ and $O(4)$, respectively. The agreement with the physical thresholds (broken lines) is clear. Moreover, we can already find indications concerning the class of critical exponents of our clusters. In fact, if one knows the critical point and the exponent ν, a rescaling of γ_r as a function of $(T - T_c)L^{1/\nu}$ should give us the same function for each lattice size (see equation (4.3)). Figures 3 and 4 show the rescaled percolation cumulant curves for $O(2)$, using $\beta_c = 0.454\,16$ and two different values of the exponent ν: the $O(2)$ value and the random percolation one, respectively.

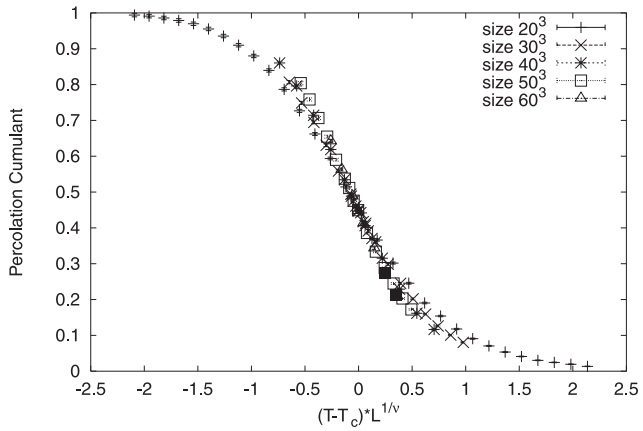

Figure 4. Rescaled percolation cumulant for $O(2)$ using $\beta_c = 0.454\,16$ and the three-dimensional random percolation exponent $\nu = 0.88$.

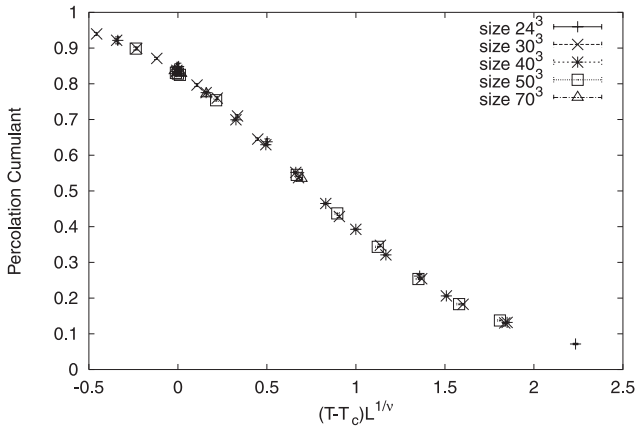

Figure 5. Rescaled percolation cumulant for $O(4)$ using $\beta_c = 0.9359$ and the $O(4)$ exponent $\nu = 0.742$.

The scaling we get in correspondence to the $O(2)$ value is remarkable. In figures 5 and 6 we repeat the same analysis for $O(4)$ ($\beta_c = 0.9359$); here it is also clear that the percolation exponent ν is in agreement with the $O(4)$ value. (We have considered values for the $O(2)$ and $O(4)$ models from [20] and [21, 22], respectively.)

To determine more precisely the critical point we have used the scaling relation (4.3) for variables S and P. By plotting $\mathcal{O}$ as a function of L at the critical temperature, we can obtain the exponent ratio ρ/ν directly from the slope of the data points on a log–log plot.

We concentrated on the critical regions that we localized through the percolation cumulant and performed more simulations for several β values looking for βs for which we get the best χ^2 for the linear fit of the data points on a log–log plot. The results for $O(2)$ and $O(4)$ are given in tables 1 and 2, respectively.

The agreement with the physical values in [20–22] is good. So far we have presented the results obtained using the first approach. The results derived using the second approach are

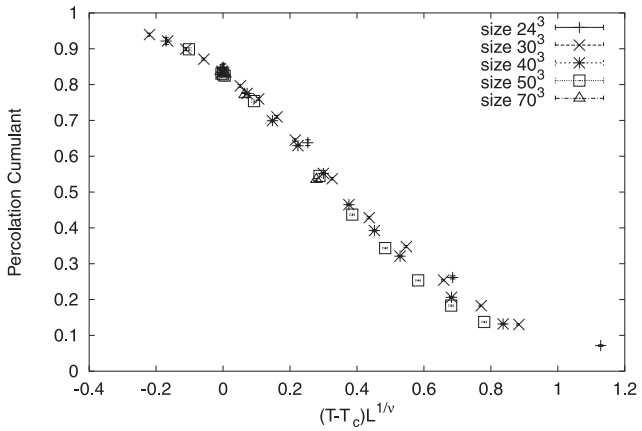

Figure 6. Rescaled percolation cumulant for $O(4)$ using $\beta_c = 0.9359$ and the three-dimensional random percolation exponent $\nu = 0.88$.

Table 1. Comparison of the thermal and percolation thresholds and exponents for $O(2)$.

	β_c	β/ν	γ/ν
Percolation results	0.454 18(2)	0.516(5)	1.971(15)
Thermal results [20]	0.454 165(4)	0.5189(3)	1.9619(5)

Table 2. Comparison of the thermal and percolation thresholds and exponents for $O(4)$.

	β_c	β/ν	γ/ν
Percolation results	0.935 95(3)	0.515(5)	1.961(15)
Thermal results	0.935 90(5) [21]	0.5129(11) [22]	1.9746(38) [22]

essentially the same; besides, we observe an improved quality of the scaling, mainly because of the use of periodic boundary conditions, which considerably reduce the finite-size effects. In particular, in figures 7 and 8 we show the scaling of S and P at the thermal thresholds reported in [20, 21]. We observe very small finite-size effects (lattices of $L \geqslant 20$ are used in the fits), especially for the $O(2)$ case, which is in contrast to what is observed for thermal observables [23]. The slopes of the straight lines are in agreement with the values of the thermal exponent ratios β/ν, γ/ν.

We thus confirm numerically the equivalence found in section 3 for the $O(2)$ case, and verify that it also holds in the $O(4)$ case.

5. Conclusions

In this work we have shown that the spontaneous breaking of the continuous rotational symmetry for the three-dimensional $O(2)$, $O(3)$ and $O(4)$ spin models can be described as percolation of Wolff clusters. For $O(2)$ and $O(3)$ the result was proven analytically, for $O(4)$ it was derived by means of lattice Monte Carlo simulations. In all cases, the number n of components of the spin vectors $\boldsymbol{s}$ does not seem to play a role; the result is thus likely to be valid for any $O(n)$ model.

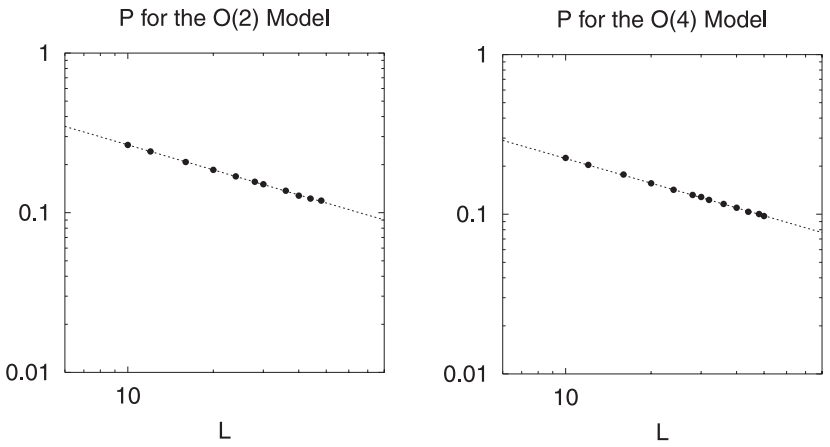

Figure 7. Finite-size-scaling plot at T_c for the percolation observable P as a function of the lattice size L. The slopes in the plots correspond to $\beta'/\nu' = 0.521(3), 0.513(6)$, respectively, for $O(2)$ and $O(4)$. Error bars are one standard deviation.

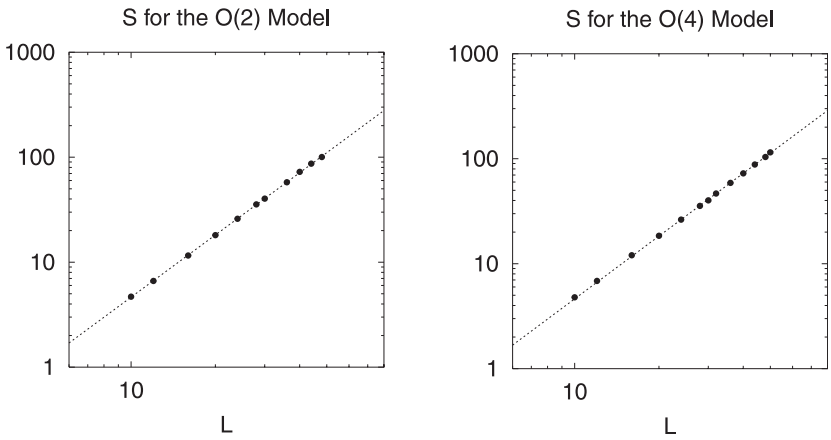

Figure 8. Finite-size-scaling plot at T_c for the percolation observable S as a function of the lattice size L. The slopes in the plots correspond to $\gamma'/\nu' = 1.97(1), 1.99(1)$, respectively, for $O(2)$ and $O(4)$. The two curves look surprisingly similar to each other. Error bars are one standard deviation.

Acknowledgments

It is a pleasure to thank J Engels for helpful discussions. We would also like to thank the TMR network ERBFMRX-CT-970122, the DFG Forschergruppe Ka 1198/4-1 and German Science Ministry BMBF under contract 06BI902 for financial support.

References

[1] Fisher M E 1967 *Physics* **3** 255–83
[2] Coniglio A and Klein W 1980 *J. Phys. A: Math. Gen.* **13** 2775
[3] Coniglio A *et al* 1977 *J. Phys. A: Math. Gen.* **10** 205–18
[4] Müller-Krumbhaar H 1974 *Phys. Lett.* A **48** 459
[5] Sykes M F and Gaunt D S 1976 *J. Phys. A: Math. Gen.* **9** 2131–7

[6] Fortuin C M and Kasteleyn P W 1972 *Physica* **57** 536
[7] Wolff U 1989 *Phys. Rev. Lett.* **62** 361
[8] Manoussakis E and Salvador R 1989 *Phys. Rev.* B **40** 2205
[9] Pisarski R and Wilczeck F 1984 *Phys. Rev.* D **29** 338
Wilczeck F 1992 *Int. J. Mod. Phys.* A **7** 3911
Rajagopal K and Wilczeck F 1993 *Nucl. Phys.* B **399** 395
[10] Chayes L 1998 *Commun. Math. Phys.* **197** 623
[11] Campbell M and Chayes L 1998 *J. Phys. A: Math. Gen.* **31** 255–9
[12] Swendsen R H and Wang J S 1987 *Phys. Rev. Lett.* **58** 86
[13] Bialas P *et al Nucl. Phys.* B **583** 368
(Bialas P *et al* 1999 *Preprint* hep-lat/9911020)
[14] Blanchard Ph, Chayes L and Gandolfo D 2000 *Nucl. Phys.* B **588** 229
[15] Griffiths R B 1969 *J. Math. Phys.* **10** 1559
[16] Fortuin C M, Kasteleyn P W and Ginibre J 1971 *Commun. Math. Phys.* **22** 89
[17] Stauffer D and Aharony A 1994 *Introduction to Percolation Theory* (London: Taylor and Francis)
[18] Binder K 1986 *Monte Carlo Methods in Statistical Physics* (Berlin: Springer)
[19] Aizenman M 1997 *Nucl. Phys.* B **485** [FS] 551
[20] Hasenbusch M and Török T 1999 *J. Phys. A: Math. Gen.* **32** 6361
[21] Oevers M 1996 *Diploma Thesis* Bielefeld University
[22] Kanaya K and Kaya S 1995 *Phys. Rev.* D **51** 2404
[23] Engels J and Mendes T 2000 *Nucl. Phys.* B **572** 289
(Engels J *et al Preprint* hep-lat/0006023)